Fluorescently-Labeled Ferrichrome Analogs as Probes for Receptor-Mediated, Microbial Iron Uptake

Haim Weizman,[†] Orly Ardon,[‡] Brenda Mester,[†] Jacqueline Libman,[†] Oren Dwir,[†] Yitzhak Hadar,*[,‡] Yona Chen,[‡] and Abraham Shanzer*[,†]

Contribution from the Department of Organic Chemistry, The Weizmann Institute of Science, and Department of Plant Pathology and Microbiology, The Hebrew University of Jerusalem, Faculty of Agriculture, Rehovot, 76100, Israel

Received April 1, 1996[⊗]

Abstract: Biomimetic analogs **1** of the microbial siderophore (iron carrier) ferrichrome were labeled with a fluorescent marker at a site which does not interfere with iron binding or receptor recognition to provide iron(III) carriers **5** and **10** (Figure 1). These carriers were built from a tetrahedral carbon as an anchor which was symmetrically extended by three converging iron-binding chains and a single, exogenous anthracenyl residue. Carriers **5** varied in the nature of the amino acids (**G** = glycyl, **A** = alanyl and **L** = leucyl) linking the anchor with the iron-binding hydroxamate groups, while the alanyl derivative **10A** differed from **5A** in the spacer between the anthracenyl label and the anchor. Examination of these binders by ^{1}H NMR confirmed that their conformations were analogous to those of the nonlabeled parent compounds. Titration experiments using UV/vis and fluorescence spectroscopy demonstrated the quenching of these compounds' fluorescence upon iron(III) loading and its recovery upon iron(III)'s release to a competing chelator. The quenching process fits the Perrin model for static quenching and was more efficient in derivatives **5**, where the label could approach the iron-binding domain, than in derivative **10A**, where the label's approach was prohibited. These data are in compliance with an intramolecular quenching process. *In vivo* examination of the labeled derivatives **5** with *Pseudomonas putida* as the indicator organism established that their behavior parallels that of the nonlabeled analogs **1**, with the added benefit of signaling microbial activity by fluorescence emission. Thus incubation of *P. putida* with iron(III)-loaded (and therefore nonfluorescent) **5G** caused buildup of the label's fluorescence in the culture medium. These observations provide direct evidence for a shuttle-mechanism of iron delivery where the fluorescent, iron-unloaded carrier is released to the medium. Inhibition of both phenomena by natural ferrichrome or NaN_3 demonstrates the involvement of the microbial ferrichrome receptor and transport systems, respectively. On the other hand, **5A** induced only modest iron(III) uptake by *P. putida* and failed to generate fluorescence in the culture medium, concurring with its action as an inhibitor. The fact that two strains of different *Pseudomonas* species did not respond to the ferrichrome analog **5G** illustrates the specificity of these compounds. The performance of these carriers as structural and functional probes, paired with their high species specificity, encourage their consideration as diagnostic tools for the detection and identification of pathogenic bacteria and fungi.

Introduction

Iron plays a crucial role in the growth and development of living systems: it functions as a catalyst in some of the most fundamental enzymatic processes, such as oxygen metabolism, electron transfer, and DNA and RNA synthesis. However, adequate iron acquisition is not a trivial task due to two major difficulties. Firstly, most of the iron in the earth's crust exists as ferric oxide, which is poorly accessible because of its low water solubility. Secondly, intracellular iron levels need to be meticulously controlled: a lack of iron causes severe deficiency symptoms, whereas excess iron may be equally harmful or even fatal. To overcome these problems, microorganisms have developed ingenious iron acquisition strategies based on the use of molecular vehicles, namely iron(III) carriers or siderophores.[1−5] These iron carriers are excreted into the environment, where they solubilize and scavenge the scarcely available iron and deliver it to the cell as siderophore−iron complexes via binding to specific membrane receptors and transport proteins.[6−13] This receptor-regulated process, in contrast to diffusion-controlled processes, enables the accumulation of iron against unfavorable concentration gradients. It should be noted that most bacteria and fungi make use of siderophores, and that most possess several siderophore receptors and transport systems, even though they produce only one siderophore. This strategy enables the organism to compete effectively for the scarcely available iron by making use of any available siderophore. To date, more than 200 siderophores have been isolated and characterized, and these have been found to vary greatly in chemical composition and topology. As a whole, they can be divided into two classes that possess either catecholates or hydroxamates as binding sites

[†] The Weizmann Institute of Science.

[‡] The Hebrew University of Jerusalem.

[⊗] Abstract published in *Advance ACS Abstracts,* November 15, 1996.

(1) Winkelmann, G.; van der Helm, D.; Neilands, J. B. *Iron Transport in Microbes, Plants and Animals*; VCH Verlagsgesellschaft mbH, D-6940: Weinheim, Germany, 1987.

(2) Neilands, J. B. *Struct. Bonding* **1984**, *58*, 1−24.

(3) Matzanke, B. F.; Müller-Matzanke, G.; Raymond, K. N. *Iron Carriers and Iron Proteins*; VCH Publishers: NY, 1989; Vol. 5, pp 1−121.

(4) Hider, R. C. *Struct. Bonding* **1984**, *58*, 25−87.

(5) Guerinot, M. L. *Annu. Rev. Microbiol.* **1994**, *48*, 743−772.

(6) Bagg, A.; Neilands, J. B. *Microbiology Rev.* **1987**, *51*, 509−518.

(7) Emery, T.; Emery, L.; Olsen, R. K. *Biochem. Biophys. Res. Commun.* **1984**, *119*, 1191−1197.

(8) Winkelmann, G. *FEBS Lett.* **1979**, *97*, 43−46.

(9) Winkelmann, G.; Braun, V. *FEBS Microbiol. Lett.* **1981**, *11*, 237−241.

(10) Neilands, J. B.; Erickson, T. J.; Rastetter, W. H. *J. Biol. Chem.* **1981**, *256*, 3831−3832.

(11) Braun, V. In *The Enzymes of Biological Membranes*; Martonosi, A. N., Ed.; Plenum Press: NY, 1985; Vol. 3, pp 617−652.

(12) Rutz, J. M.; Liu, J.; Lyons, J. A.; Goranson, J.; Armstrong, S. K.; McIntosh, M. A.; Feiz, J. B.; Klebba, P. E. *Science* **1992**, *258*, 471−475.

(13) Killmann, H.; Benz, R.; Braun, V. *EMBO J.* **1993**, *12*, 30007−30016.

S0002-7863(96)01064-5 CCC: $12.00

and into three topological families that assume tripodal, macrocyclic, or linear shapes.[14,15] Regardless of their composition or topology, they all are hydrophilic and function by the same principles: they bind iron highly effectively by embedding it into an octahedral ion-binding cavity and generate a molecular envelope which fits the respective membrane receptor.

The importance and ingenuity of these iron-acquisition processes prompted us to consider all artificial siderophore analogs as structural probes of microbial iron uptake processes.[16,17] To provide prototypical structures, we selected as targets siderophore analogs that span both chemical classes, catecholates and hydroxamates, and that include two of the three topologies, tripodal and linear. Applying the principles of biomimetic chemistry,[18] we thus synthesized analogs of enterobactin (tripodal catecholate),[19] ferrichrome (tripodal hydroxamate),[20] and ferrioxamine and coprogen (linear hydroxamates),[21] and examined their behavior both *in vitro* and *in vivo*. For the *in vivo* studies, *Pseudomonas putida* was used as the indicator organism. *P. putida* possesses the desired range of siderophore receptors, including those for ferrichrome, ferrioxamine, and coprogen, whose responses to each of the siderophore analogs can be readily tested and compared with that of other organisms. These studies led us to identify ferrichrome[22,23] (**1** in Figure 1) as well as ferrioxamine analogs[24,25] that distinguish between analogous receptors of different organisms,[17,22] specifically analogous receptors of *P. putida*, *Arthrobacter flavescens*, and *Erwinia herbicola*. The strikingly high species specificity of some of the synthetic analogs is in contrast to the behavior of the natural carriers, which do not distinguish between related receptors of different organisms. This outstanding feature of synthetic carriers encouraged us to examine their potential as diagnostic tools for the detection and identification of specific microorganisms.

To this aim we labeled the bioactive carriers with fluorescent markers, to monitor their microbial activity. The use of fluorescent markers appeared promising because of the established versatility of fluorescently labeled alkali- and alkaline-earth metal-ion binders for *in vivo* studies of ion fluxes,[26] and the recent reports on fluorescently labeled binders for the detection of iron[27−29] and of other metal ions, including copper and nickel.[30−33] Moreover, studies from our laboratories have demonstrated the potential of fluorescently labeled natural siderophores for the investigation of iron exchange processes.[34−37]

Here we introduce bioactive ferrichrome analogs that are labeled with anthracene as the fluorescent marker at a site which interferes neither with iron binding nor receptor recognition. We describe the design, synthesis, structures, and iron(III)-binding properties of fluorescently labeled analogs **5** and **10**. We demonstrate that these compounds adopt the same conformations as their parent congeners, both in the free state and as their iron(III) complexes. We confirm that they convert from a fluorescent to a nonfluorescent state when binding iron(III) and that they regain their fluorescence upon iron(III)'s release to a competing chelator. We further report on the *in vivo* behavior of these analogs **5** (Figure 1). We demonstrate that the activity of these compounds as iron(III) carriers to *P. putida* indeed parallels that of the nonlabeled parent compounds, with the added benefit of signaling microbial iron(III) uptake via the appearance of the compound's fluorescence in the culture medium. We also illustrate the strong specificity of these compounds, which failed to recognize two strains of a different *Pseudomonas* species.

Experimental Procedures, Materials and Methods[38]

Synthesis of Fluorescent Ferrichrome Derivatives 5G, 5A, and 5L. Synthesis of Tetraphenolate C($CH_2OCH_2CH_2COOC_6Cl_5$)$_4$ (2). Pentaerythritol (9.53 g, 0.07 mol) was treated dropwise with NaOH (0.7 mL of 30% w/w) and then with acrylonitrile (20.3 mL, 0.44 mol) such that the temperature did not exceed 30 °C. The mixture was stirred overnight at room temperature, then neutralized with 1 N HCl, extracted into EtOAc (200 mL), washed twice with water, dried over Na_2SO_4, and concentrated to yield 22.9 g (0.0657 mol, 94% yield) of tetranitrile. Tetranitrile (7.22 g, 0.021 mol) was treated with concentrated HCl (10 mL), stirred for 4 h at 95 °C, extracted into cold EtOAc (300 mL), washed twice with water, dried over Na_2SO_4, and concentrated to yield 6.67 g (15.7 mmol, 75% yield) tetra acid. Tetra acid (11.5 g, 0.027 mol) was treated with $SOCl_2$ (11.9 mL, 0.163 mol) overnight at 40 °C. Excess thionyl chloride was distilled to provide a crude tetraacyl halide. Crude tetraacyl chloride was dissolved in dry $CHCl_3$, and pentachlorophenol (28.76 g, 0.108 mol) was added. The mixture was cooled to 0 °C, treated with Et_3N (15 mL, 0.108 mol), and then stirred at room temperature. After the reaction was completed according to IR, the mixture was concentrated and purified by flash chromatography (silica gel, $CHCl_3$). Residual pentachlorophenol was removed by filtration over deactivated neutral alumina to yield 11.94 g (8.42 mmol, 31% yield) of tetrapentachlorophenolate. IR ($CDCl_3$) ν 1783 cm^{-1} ($COOC_6Cl_5$). ^{1}H NMR 80 MHz, $CDCl_3$ δ 3.81 (t, J = 6 Hz, 8H, CCH_2OCH_2), 3.46 (s, 8H, CCH_2O), 2.91 (t, J = 6 Hz, 8H, CH_2CN).

Synthesis of 9(Aminomethyl)anthracene (4). A solution of 9-anthracenecarbonitrile (8.13 g, 0.04 mol) and $NaBH_4$ (1.02 g, 0.027 mol) in dry THF (100 mL, distilled over Na) was treated dropwise for over 1 h with BF_3·Et_2O (4.43 mL, 0.036 mol in 10 mL of THF). After

(14) van der Helm, D.; Jalal, M. A. F.; Hossain, M. B. In *Iron Transport in Microbes, Plants and Animals*; Winkelmann, G., van der Helm, D., Neilands, J. B., Eds.; VCH Verlagsgesellschaft mbH, D-69451: Weinheim, Germany, 1987; pp 135−166.
(15) Jalal, M. A. F.; van der Helm, D. In *Handbook of Microbial Iron Chelates*; Winkelmann, G., Ed.; CRC Press: Boca Raton, Ann Arbor, Boston, London, 1991; pp 235−269.
(16) Shanzer, A.; Libman, J. In *Handbook of Microbial Iron Chelates*; Winkelmann, G., Ed.; CRC: Boca Raton, Ann Arbor, Boston, London, 1991; pp 309−338.
(17) Shanzer, A.; Libman, J; Yakirevitch, P.; Hadar, Y.; Chen, Y.; Jurkevitch, E. *Chirality* **1993**, *5*, 359−365.
(18) Breslow, R. *Chem. Soc. Rev.* **1972**, *1*, 553−580.
(19) Tor, Y.; Libman, J.; Shanzer, A.; Felder, C. E.; Lifson, S. *J. Am. Chem. Soc.* **1992**, *114*, 6661−6671.
(20) Dayan, I.; Libman, J.; Agi, Y.; Shanzer, A. *Inorg. Chem.* **1993**, *32*, 1467−1475.
(21) Yakirevitch, P.; Rochel, N.; Albrecht-Gary, A.-M.; Libman, J.; Shanzer, A. *Inorg. Chem.* **1993**, *32*, 1779−1787.
(22) Shanzer, A.; Libman, J; Lazar, R.; Tor, Y.; Emergy, T. *Biochem. Biophys. Res. Commun.* **1988**, *157*, 389−394.
(23) Jurkevitch, E.; Hadar, Y.; Chen, Y.; Libman, J.; Shanzer, A. *J. Bacteriol.* **1992**, *174*, 78−83.
(24) Berner, I.; Yakirevitch, P.; Libman, J.; Shanzer, A.; Winkelmann, G. *Biol. Metals* **1991**, *4*, 186−191.
(25) Jurkevitch, E.; Hadar, Y.; Chen, Y.; Yakirevitch, P.; Libman, J.; Shanzer, A. *Microbiology-UK* **1994**, *140*, 1697−1703.
(26) Tsien, R. Y. *Ann. Rev. Neurosci.* **1989**, *12*, 227−253.
(27) Bodenant, B.; Fages, F. *Tetrahedron Lett.* **1995**, *36*, 1451−1454.
(28) Barrero, M.; Cámara, C.; Pérez-Conde, M. C.; José, C. S.; Fernández, L. *Analyst* **1995**, *120*, 431−435.
(29) Barrero, J. M.; Morenobondi, M. C.; Pérez-Conde, M. C.; Cámara, C. *Talanta* **1993**, *40*, 1619−1623.
(30) Czarnik, A. W. *Acc. Chem. Res.* **1994**, *27*, 302−308.
(31) Bissell, R. A.; Silva, A. P. d.; Gunaratne, H. Q. N.; Lynch, P. L. M.; Maguire, G. E. M.; Sandanayake, K. R. A. S. *Chem. Soc. Rev.* **1992**, *21*, 187−195.
(32) Fabbrizzi, L.; Licchelli, M.; Pallavicini, P.; Perotti, A.; Sacchi, D. *Angew. Chem., Int. Ed. Engl.* **1994**, *33*, 1975−1977.
(33) Fabbrizzi, L.; Poggi, A. *Chem. Soc. Rev.* **1995**, *24*, 197−202.
(34) Lytton, S. D.; Cabantchik, Z. I.; Libman, J.; Shanzer, A. *Mol. Pharmacol.* **1991**, *40*, 584−590.
(35) Lytton, S. D.; Mester, B.; Libman, J.; Shanzer, A.; Cabantchik, Z. I. *Anal. Biochem.* **1992**, *205*, 326−333.
(36) Bar-ness, E.; Hadar, Y.; Chen, Y.; Shanzer, A.; Libman, J. *Plant Physiol.* **1992**, *99*, 1329−1335.
(37) Loyevsky, M.; Lytton, S. D.; Mester, B.; Libman, J.; Shanzer, A.; Cabantchik, Z. I. *J. Clin. Investigations* **1993**, *91*, 218−224.
(38) The molar extinction coefficients ϵ are given in units of 10^3 cm^2 M^{-1}, and the circular dichroism values $\Delta\epsilon$, defined as $\epsilon_L - \epsilon_R$, are given in units of 10^3 cm^2.

stirring for an additional hour at room temperature, excess hydride was destroyed by adding concentrated HCl. The reaction mixture was concentrated to dryness, and 1 N NaOH (40 mL) was added. The compound was extracted into $CHCl_3$ (400 mL), concentrated, and purified by flash chromatography (silica gel, 0−4% MeOH/$CHCl_3$) to provide 536 mg (2.59 mmol, 7% yield) of product with a mp of 98−100 °C. ^{1}H NMR 400 MHz, CD_3OD δ 8.45 (s, 1H, Ar*H*), 8.38 (d, J = 8.88 Hz, 2H, Ar*H*), 8.04 (d, J = 8.4 Hz, 2H, Ar*H*), 7.56 (t, J = 7.2 Hz, 2H, Ar*H*), 7.48 (t, J = 7.4 Hz, 2H, Ar*H*), 4.79 (m, 2H, Ant*CH*$_2$). UV/vis ($CHCl_3$)-λ_{max} = 334, 350, 368, and 389 nm, ϵ = 2906, 5744, 8719, and 783.

Synthesis of Ferrichrome Analog (5G). $C_{14}H_9$-$CH_2NHCOCH_2$-$CH_2OCH_2C(CH_2OCH_2CH_2CONHCH_2CON(OH)CH_3)_3$. Tetra active ester (**2**) (1.29 g, 0.91 mmol) and $H_2NCH_2CON(OH)CH_3$ (**3**) (592 mg, 2.73 mmol) were dissolved in 100 mL of dry chloroform, and then 9-(aminomethyl)anthracene (**4**) (186 mg, 0.91 mmol) was added. The solution was stirred overnight while maintaining pH ∼ 8 with Et_3N. The solution was concentrated and flash-chromatographed over silica gel (0−15% MeOH−$CHCl_3$). The compound was further purified on PLC (**P**reparative **L**ayer **C**hromatography) (9% MeOH−$CHCl_3$) to give 110 mg (14% yield) of product. IR ($CDCl_3$) ν 1634 cm^{-1} (CONH, CONOH) ^{1}H NMR 400 MHz, CD_3OD δ 8.49 (s, 1H, Ar*H*), 8.35 (d, J = 8.6 Hz, 2H, Ar*H*), 8.03 (d, J = 8.2 Hz, 2H, Ar*H*), 7.55 (m, 2H, Ar*H*), 7.48 (m, 2H, Ar*H*), 5.38 (s, 2H, AntCH_2), 4.10 (s, 2H, NH*CH*$_2$), 3.59 (m, 2H, CH_2O), 3.30 (m, 8H, OCH_2C + O*CH*$_2CH_2$), 3.17 (s, 9H, NCH_3), 2.94 (s, 6H, C*CH*$_2$O), 2.40 (t, J = 4.9 Hz, 2H, $COCH_2$), 2.32 (t, J = 5.6 Hz, 6H, CH_2CO). FAB MS 925.54 (M + Fe − 2H)$^+$, 894.54 (M + Na)$^+$, 872.53 (M + H)$^+$. Fe(III) complex: UV/vis λ_{max} 426 nm, ϵ = 2760.

Synthesis of Ferrichrome Analog (5A). $C_{14}H_9$-$CH_2NHCOCH_2$-$CH_2OCH_2C(CH_2OCH_2CH_2CONHCH(CH_3)CON(OH)CH_3)_3$. Tetraphenolate $C(CH_2OCH_2CH_2COOC_6Cl_5)_4$ (**2**) (1.418 g, 1 mmol), 9-(aminomethyl)anthracene (**4**) (207 mg, 1 mmol), $H_2NCH(CH_3)CON(OH)CH_3$ (**3**) (354 mg, 3 mmol), and imidazole (30 mg) in dry $CHCl_3$ (20 mL) were stirred for 2 days at room temperature (maintaining pH ∼ 8 by addition of Et_3N). The reaction mixture was concentrated and purified by flash chromatography (silica gel) (0−6% MeOH−$CHCl_3$) to yield 183 mg (0.2 mmol, 20% yield) of the desired product. IR ($CDCl_3$) ν 1632 cm^{-1} (CONH, CONOH). ^{1}H NMR 400 MHz, $CDCl_3$ δ 10.15 (br, 3H, OH), 8.46 (s, 1H, Ar*H*), 8.31 (d, J = 8.3 Hz, 2H, Ar*H*), 8.03 (d, J = 8.3 Hz, 2H, Ar*H*), 7.55 (m, 2H, Ar*H*), 7.49 (m, 2H, Ar*H*), 7.25 (*NH*CαH), 6.93 (m, 1H, CH_2*NH*), 5.43 (d of ABq, J_1 = 28 Hz, J_2 = 14.5 Hz, J_3 = 4.8 Hz, 2H, Ant*CH*$_2$), 5.04 (m, 3H, Cα*H*), 3.60 (m, 2H, CH_2O), 3.25 (br, 8H, *CH*$_2$C + OCH_2) 3.19 (s, 9H, NCH_3) 2.85 (ABq, J_1 = 29 Hz, J_2 = 8.9 Hz, 6H, CCH_2O), 2.49 (m, 2H, $COCH_2$), 2.29 (m, 3H, CH_2CO), 2.17 (m, 3H, CH_2CO), 1.32 (d, J = 6.8 Hz, 9H, CαH*CH*$_3$). FAB MS 914.22 (M + H)$^+$. Fe(III) complex: UV/vis λ_{max} 425 nm, ϵ = 2610. CD λ_{ext} 368, 422, 453 nm, $\Delta\epsilon$ = −4.5, 0.0, +1.8.

Synthesis of Ferrichrome Analog (5L). $C_{14}H_9$-$CH_2NHCOCH_2$-$CH_2OCH_2C(CH_2OCH_2CH_2CONHCH(C_4H_9)CON(OH)CH_3)_3$. Tetraphenolate $C(CH_2OCH_2CH_2COOC_6Cl_5)_4$ (709 mg, 0.5 mmol), 9-(aminomethyl)anthracene (103 mg, 0.5 mmol), H_2NCH(iBu)$CON(OH)CH_3$ (240 mg, 1.5 mmol), and imidazole (15 mg) in dry $CHCl_3$ (15 mL) were stirred for 2 days at room temperature (maintaining pH ∼ 8 by addition of Et_3N). The reaction mixture was concentrated and purified by flash chromatography (silica gel, 0−4% MeOH/$CHCl_3$) to yield 68 mg (0.065 mmol, 13 % yield) of product. IR ($CDCl_3$) ν 1632 cm^{-1} (CONH,CONOH). ^{1}H NMR 400 MHz, CD_3OD δ 8.52 (s, 1H, Ar*H*), 8.37 (d, J = 8.3 Hz, 2H, Ar*H*), 8.05 (d, J = 8.4 Hz, 2H, Ar*H*), 7.56 (m, 2H, Ar*H*), 7.49 (m, 2H, Ar*H*), 6.93 (m, 1H, CH_2*NH*), 5.42 (s, 2H, Ant*CH*$_2$), 5.11 (m, 3H, C_αH) 3.60 (t, J = 5.8 Hz, 2H, CH_2*CH*$_2$O), 3.32 (m, 6H, O*CH*$_2CH_2$), 3.18 (s, 2H, OCH_2C), 3.16 (s, 9H, NCH_3), 2.98 (s, 6H, CCH_2O), 2.46 (m, 2H, $COCH_2$), 2.29 (m, 6H, CH_2CO), 1.65 (m, 3H, CH{*iBu*}), 1.53 (m, 6H, CH_2{*iBu*}) 0.92 (m, 18H, CH_3{*iBu*}). Fe(III) complex: UV/vis λ_{max} 425 nm, ϵ = 2800. CD λ_{ext} 365, 412, 443 nm, $\Delta\epsilon$ = −5.2, 0.0, +2.5.

Synthesis of Ferrichrome Analog 10A. Ant-$CH_2SCH_2(CH_2OCH_2CH_2CN)_3$ (7). A solution of thiol (3.43 g, 22.5 mmol),[39] 9-(chloromethyl)anthracene (5.1 g, 22.5 mmol), and $NaHCO_3$ (3.78 g, 45 mmol) in DMF (20 mL) was stirred overnight at room temperature under argon. The DMF was removed under high vacuum, and the residue was dissolved in $CHCl_3$ (200 mL). The solution was washed with water, dried over Na_2SO_4, and concentrated. Chromatography over silica gel (50−80% EtOAc−hexane) yielded 1.69 g of *ant*-CH_2-$SCH_2(CH_2OH)_3$ (4.95 mmol, 22% yield). ^{1}H NMR 270 MHz CD_3OD δ 8.43 (s, 1H, Ar*H*), 8.41 (d, J = 1.3 Hz, 2H, Ar*H*), 8.02 (d, J = 9.5 Hz, 2H, Ar*H*), 7.54−7.45 (m, 4H, Ar*H*), 4.83 (s, 2H, Ant-CH_2S), 3.64 (s, 6H, CH_2OH), 2.93 (s, 2H, SCH_2C).

Ant-$CH_2SCH_2(CH_2OH)_3$ (1.69 g, 4.95 mmol) was treated with NaOH (50 mL of 30% w/w) and then added dropwise with acrylonitrile (1.3 mL, 19.8 mmol). The reaction mixture was stirred overnight, dissolved in $CHCl_3$, and washed with 1 N HCl and water. Concentration and purification over silica gel (CH_2Cl_2) yielded 1.6 g of **7** (3.2 mmol, 64.7% yield). IR ($CDCl_3$) ν 2254 cm^{-1} (CN), 1118 cm^{-1} (CH_2OCH_2). ^{1}H NMR 270 MHz $CDCl_3$ δ 8.41 (s, 1H, Ar*H*), 8.34 (d, J = 9.6 Hz, 2H, Ar*H*), 7.99 (d, J = 7.9 Hz, 2H, Ar*H*), 7.58 (m, 2H, Ar*H*), 7.47 (m, 2H, Ar*H*), 4.77 (s, 2H, Ant-CH_2S), 3.56 (t, J = 6 Hz, 6H, CH_2O*CH*$_2$), 3.39 (s, 6H, *CH*$_2OCH_2$), 2.85 (s, 2H, SCH_2C), 2.50 (t, J = 6 Hz, CH_2CN).

Ant-$CH_2SO_2CH_2(CH_2OCH_2CH_2COOCH_3)_3$ (8). A cold solution (0 °C) of **7** (721 mg, 1.44 mmol) in dry CH_2Cl_2 (50 mL) was treated with 3-chloroperbenzoic acid (680 mg of 80% pure, 3.95 mmol) for 10 min. The reaction mixture was diluted with CH_2Cl_2, washed with water and 0.1 N NaOH, dried over Na_2SO_4, and concentrated. Purification over silica gel (0−1% MeOH−CH_2Cl_2) yielded 523 mg of Ant-$CH_2SO_2CH_2(CH_2OCH_2CH_2CN)_3$ (0.98 mmol, 68% yield). IR ($CDCl_3$) ν 2254 cm^{-1} (CN), 1313 cm^{-1} (SO_2), 1114 cm^{-1} (CH_2OCH_2), 1018 cm^{-1} (SO_2). ^{1}H NMR 400 MHz $CDCl_3$ δ 8.55 (s, 1H, Ar*H*), 8.35 (d, J = 8.9 Hz, 2H, Ar*H*), 8.05 (m, 2H, Ar*H*), 7.65 (m, 2H, Ar*H*), 7.52 (m, 2H, Ar*H*), 5.43 (s, 2H, Ant-*CH*$_2SO_2$), 3.60 (s, 6H, *CH*$_2OCH_2$), 3.57 (t, J = 6 Hz, 6H, CH_2O*CH*$_2$), 3.35 (s, 2H, SO_2CH_2C), 2.45 (t, J = 6 Hz, CH_2CN).

The trinitrile (608 mg, 1.41 mmol) was dissolved in a saturated solution of HCl in dry MeOH (3 mL). The solution was heated under reflux for 2 h and then stirred overnight at room temperature. The solution was then concentrated, dissolved in CH_2Cl_2, washed with saturated $NaHCO_3$ and water, and dried over Na_2SO_4. Purification over silica gel (0−1% MeOH−CH_2Cl_2) yielded 455 mg of **8** (0.72 mmol, 51% yield). IR ($CDCl_3$) ν 1736 cm^{-1} ($COOCH_3$). ^{1}H NMR 400 MHz $CDCl_3$ δ 8.54 (s, 1H, Ar*H*), 8.36 (d, J = 8.2 Hz, 2H, Ar*H*), 8.04 (d, J = 8.4 Hz, 2H, Ar*H*), 7.62 (m, 2H, Ar*H*), 7.50 (m, 2H, Ar*H*), 5.42 (s, 2H, Ant-*CH*$_2SO_2$), 3.653 (s, 9H, $COOCH_3$), 3.647 (t, J = 6.3 Hz, 6H, CH_2O*CH*$_2$), 3.56 (s, 6H, *CH*$_2OCH_2$), 3.39 (s, 2H, SO_2CH_2C), 2.49 (t, J = 6.3 Hz, CH_2COO).

Ant-$CH_2SO_2CH_2(CH_2OCH_2CH_2COOC_6Cl_5)_3$ (9). The triester **8** (455 mg, 0.72 mmol) was dissolved in EtOH (3 mL), and NaOH (3 mL of 12% w/w) was added. The reaction mixture was stirred at room temperature for 36 h and then EtOH was removed. The solution was acidified to pH 2 with 10% HCl. A brown precipitate was formed which was dissolved in $CHCl_3$. Concentration of the solution yielded 347 mg (0.59 mmol, 82% yield) of the triacid. IR ($CDCl_3$) ν 1715 cm^{-1} (COOH). ^{1}H NMR 400 MHz ($CDCl_3$−5% CD_3OD) δ 8.38 (s, 1H, Ar*H*), 8.22 (d, J = 8.8 Hz, 2H, Ar*H*), 7.90 (d, J = 8.4 Hz, 2H, Ar*H*), 7.53 (m, 2H, Ar*H*), 7.42 (m, 2H, Ar*H*), 5.29 (s, 2H, Ant-*CH*$_2SO_2$), 3.56 (t, J = 5.8 Hz, 6H, CH_2O*CH*$_2$), 3.48 (s, 6H, *CH*$_2OCH_2$), 3.33 (s, 2H, SO_2CH_2C), 2.43 (t, J = 5.8 Hz, CH_2COOH).

A cooled (0 °C) solution of triacid (308 mg, 0.52 mmol), DMAP (5 mg), and C_6Cl_5OH (416 mg, 1.56 mmol) in dry THF (20 mL) was treated with dicyclohexyl carbodiimide (321 mg, 1.56 mmol). The solution was stirred for 1 day at room temperature, and then the precipitated urea was filtered. The filtrate was concentrated and purified by chromatography over silica gel ($CHCl_3$) to yield 197 mg of **9** (0.147 mmol, 29% yield). IR ($CDCl_3$) ν 1784 cm^{-1} ($COOC_6Cl_5$). ^{1}H NMR 400 MHz $CDCl_3$ δ 8.50 (s, 1H, Ar*H*), 8.29 (d, J = 8.3 Hz, 2H, Ar*H*), 8.00 (d, J = 8.4 Hz, 2H, Ar*H*), 7.57 (m, 2H, Ar*H*), 7.48 (m, 2H, Ar*H*) 5.37 (s, 2H, Ant-*CH*$_2SO_2$), 3.76 (t, J = 6.0 Hz, 6H, CH_2O*CH*$_2$), 3.62 (s, 6H, *CH*$_2OCH_2$), 3.38 (s, 2H, SO_2CH_2C), 2.80 (t, J = 6.0 Hz, CH_2-COOH).

Ant-$CH_2SO_2CH_2(CH_2OCH_2CH_2CONHCH(CH_3)CON(OH)CH_3)_3$ (10). Triphenolate **9** (180 mg, 0.135 mmol) and $H_2NCH(CH_3)$-$CON(OH)CH_3$, **3A** (64 mg, 0.54 mmol), were dissolved in dry $CHCl_3$

(39) Tunaboylu, K.; Schwarzenbach, G. *Helv. Chim. Acta* **1971**, *54*, 2166−2184.

Scheme 1

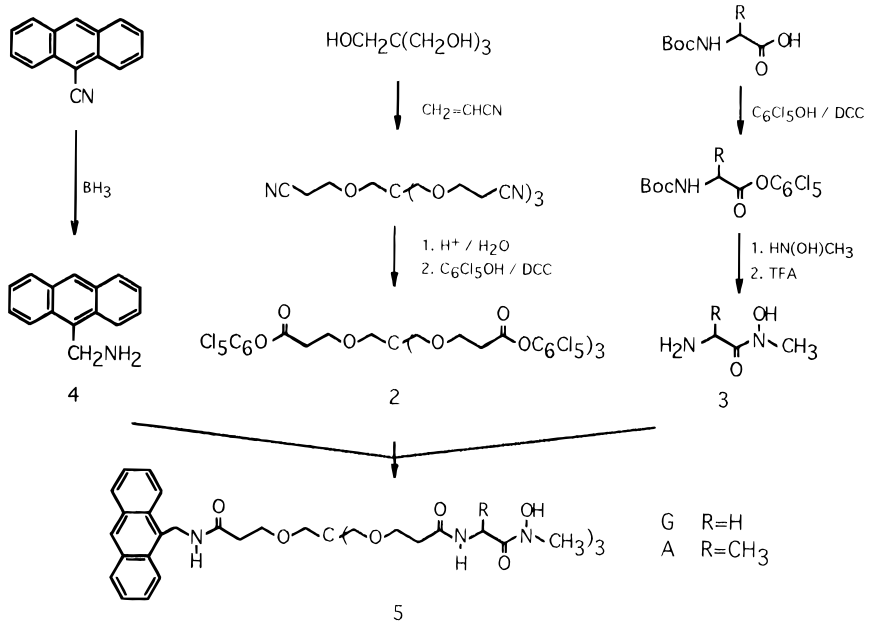

(10 mL) and stirred overnight at room temperature (maintaining pH ~ 8 by addition of Et_3N). The reaction mixture was concentrated, washed with 1 N HCl and water, and dried over Na_2SO_4. Purification by flash chromatography (0−4% MeOH/$CHCl_3$) yielded 40 mg (0.045 mmol, 33% yield) of product **10**. IR ($CDCl_3$) ν 1637 cm^{-1} (CONH, CONOH). ^1H NMR 400 MHz $CDCl_3$ δ 8.53 (s, 1H, Ar*H*), 8.42 (d, J = 8.9 Hz, 2H, Ar*H*), 8.03 (d, J = 8.3 Hz, 2H, Ar*H*), 7.61 (m, 2H, Ar*H*), 7.56 (m, 3H, *NH*C_αH), 7.49 (m, 2H, Ar*H*), 5.49 (ABq, J_1 = 48 Hz, J_2 = 14.6 Hz, 2H, Ant*CH*$_2$), 5.14 (m, 3H, C_αH), 3.54 (m, 6H, OCH_2), 3.43 (ABq, J_1 = 32 Hz, J_2 = 13.8 Hz, 2H, CH_2O), 3.41 (ABq, J_1 = 20 Hz, J_2 = 11.0 Hz, 6H, CCH_2O), 3.19 (s, 9H, NCH_3), 2.49 (m, 3H, CH_2CO), 2.25 (m, 3H, CH_2CO), 1.38 (d, J = 6.8 Hz, 9H, $C_\alpha HCH_3$). FAB MS 974.41 $(M + Fe - H)^+$, 891.45 $(M + H)^+$. Fe(III) complex: UV/vis λ_{max} 432 nm, ϵ = 2850. CD λ ext 358, 373, 387, 431, 456 nm, $\Delta\epsilon$ = −4.5, −5.3, −5.1, 0.0, +1.1.

Ligand Titration with Ferric Ions. Aliquots of stock solutions of the ligands **5L**, **5A**, **5G**, or **10A** and increasing amounts of $FeCl_3$ (both in spectroscopic grade methanol) were mixed, and after 15 min diluted with methanol/0.1 N aqueous NaOAc[40] (4/1) to a constant ligand concentration of 0.3 mM for UV/vis titrations, and of 6 μM for fluorescence titration. Measurements were performed after equilibration for 24 h at room temperature. UV/vis absorption spectra were recorded on a Hewlett-Packard diode array 8450A spectrophotometer, and fluorescence spectra were recorded on a Shimadzu RF-540 spectrofluorometer.

Bacterial Strains and Growth Conditions. The sid$^-$ mutants *Pseudomonas putida* JM218, *Pseudomonas fluorescens* S680, and *Pseudomonas fluorescens* WCS 3742 were provided by L. C. van Loon, Utrecht, The Netherlands. Such mutants are ideal for the study of Fe-siderophore utilization, since the absence of native siderophores eliminates possible interference through ligand exchange.

Bacteria were grown in LMKB medium[41] overnight at 28 °C on a rotary shaker at 180 RPM. The bacterial cultures were then centrifuged for 15 min at 2500 RPM, resuspended in fresh half-strength standard succinate medium (SSM) to a final $o.d._{620}$ of 0.6, and incubated for 60 min in a water bath at 28 °C. When appropriate, NaN_3 was added to a final concentration of 5 mM 30 min prior to the addition of the siderophores.

Microbial ^{55}Fe Uptake Studies. ^{55}Fe uptake studies were conducted according to Jurkevitch *et al.*[25] with minor modifications. The labeled ^{55}Fe-siderophore complex was added to a final concentration of 1 μM. Aliquots (0.5 mL) were taken in duplicate, layered onto a mixture of dibutyl/octyl phthalate (1/1, v/v Sigma), and centrifuged. The supernatant was removed, and the Eppendorf tube tips were cut. Radioactivity in the tips of the tubes containing the bacterial cells was counted on a Beckman LS1801 counter.

Fluorescence Studies. The Fe-siderophore complex was added to the bacterial suspension to a final concentration of 5 μM. Aliquots of 1 mL were centrifuged, and the supernatant was collected. Fluorescence was measured in an SLM Instruments fluorometer (Model 4800).

Results and Discussion

Design and Synthesis. To obtain ferrichrome analogs that could serve as diagnostic tools, we attached a chemically inert fluorescent marker to the bioactive glycyl **1G** (R = H) and alanyl **1A** (R = Me) derivatives (Figure 1), at a site that does not interfere with receptor binding.[22,23] These two congeners were selected because they had previously been proven to act as agonist[42] and antagonist,[42] respectively, towards *P. putida*.[23] The glycyl derivative **1G** fully mimicks the natural ferrichrome as an iron(III) carrier and growth promoter, whereas the alanyl derivative **1A** inhibits the action of the natural iron(III) carrier by competing for a specific site in the uptake system. We selected a fluorescent marker as a label because fluorescently labeled ferrioxamines have been shown to provide powerful probes for iron(III)-exchange processes.[35,43] We specifically chose anthracene as the label because it combines chemical inertness with highly intense absorption, high fluorescence yield, and short singlet lifetime.[44] Moreover, the absorption wavelength of anthracene does not overlap with those of ferrichydroxamate[45] or the bacterial culture. These spectral characteristics enabled both *in vitro* monitoring of iron(III)-binding and fluorescence quenching and *in vivo* follow-up of the microbial iron(III) uptake process. The fulfillment of these

(40) We used NaOAc buffer to maintain the solutions' pH values at 7.4. The use of other buffers that would have been superior for this pH range was prohibited either because they quench the probes' fluorescence (amino groups containing buffers) or because they compete with the ligands for iron(III) (phosphate buffers).

(41) King, E. O.; Ward, M. K.; Raney, D. E. *J. Lab. Clin. Med.* **1954**, *44*, 301−307.

(42) Here we use the term "agonist" for a siderophore analog that fully mimics the natural compound by acting as a microbial iron(III) carrier, and the term "antagonist" for a siderophore analog that inhibits the action of the natural compound by competitively binding to the receptor.

(43) Weizman, H. M.Sc. Thesis, Feinberg Graduate School, The Weizmann Institute of Science, 1993.

(44) Birks, J. B. *Photophysics of Aromatic Molecules*; Wiley-Interscience: London, New York, Sydney, Toronto, 1970.

(45) Raymond, K. N.; Mueller, G.; Matzanke, B. F. *Top. Cur. Chem.* **1984**, *123*, 49−102.

Scheme 2

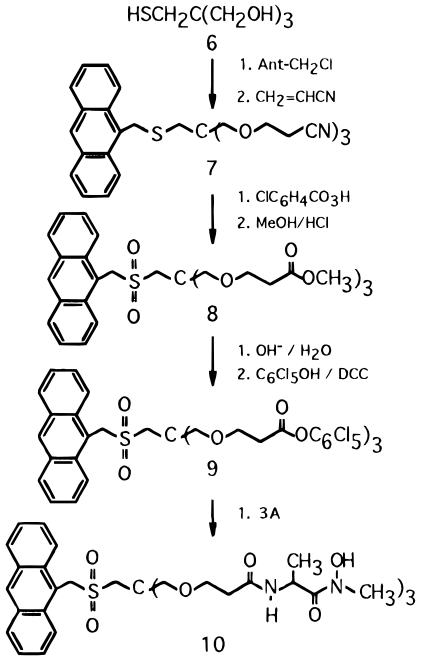

requirements was crucial since other labels, such as the weakly fluorescent quinoline, failed to provide reliable results. As an attachment point for the label we selected the carbon anchor of the ferrichrome analogs **1**. Attachment to this site was expected to not interfere with iron(III) binding or with recognition by ferrichrome-specific membrane receptors (such as the FhuA receptor in *E. coli*), as receptor recognition has been shown to occur around the iron(III)-binding domain.[22,23] For *in vitro* comparison, we also prepared the leucyl derivative **5L** and the alanyl derivative **10A**. Derivative **5L**, with its bulky side chain, was chosen to establish whether steric screening of the iron-binding domain would influence its quenching efficiency. Derivative **10A**, with the anthracene attached via a shorter linker, was chosen to trace the effect of the proximity between the label and iron(III) on the quenching process.

Synthesis of the labeled compounds **5** involved coupling of the C_3-symmetric tetraphenolate **2** with 3 equiv of hydroxamate bearing amino acid residues **3**[20] and 1 equiv of aminomethyl-anthracene **4** (Scheme 1). The sulfon derivative **10A** was prepared by coupling the labeled tris-phenolate **9** with the hydroxamate-bearing alanyl residue **3A** (Scheme 2).

Table 1. ^{1}H NMR Shift Differences [$\Delta(\delta^{5,10}-\delta^{1})$] between the Fluorescently Labeled Ligands **5** and **10** and Their Parent Ligands **1**

ligand	C-CH_2O	OCH_2	CH_2CO	NCH_3
5G CD_3OD	−0.26	−0.34	−0.17	0.00
5A $CDCl_3$	−0.32	−0.33	−0.23, −0.16	−0.07
5A CD_3OD	−0.33	−0.23	−0.17	+0.10
5L $CDCl_3$	−0.32	+0.02	−0.21, −0.17	−0.12
5L CD_3OD	−0.21	−0.27	−0.14	−0.08
10A $CDCl_3$	+0.24	−0.04	−0.03, −0.08	−0.07
10A CD_3OD	+0.38	+0.05	0.00	−0.03

Structures and Iron(III)-Binding Properties.[38] The structures of all the ferrichrome analogs were confirmed by their spectroscopic properties, such as IR, NMR, UV, and FAB MS. The ^{1}H NMR data were particularly useful, providing information on the compounds conformation and the average location of the fluorescent label relative to the iron(III)-binding domain. Three parameters were compared: (i) the number of sets of signals, to establish binders symmetry; (ii) the extent of nonequivalence of the diastereotopic protons, to estimate the ligands' conformational constraints; and (iii) the chemical shifts of the binders' backbone protons in comparison with those of the parent ligands, to assess the extent to which the anthracene label could approach the ion-binding cavity.

Table 1 highlights the differences in chemical shifts between the labeled derivatives **5** and **10** and the nonlabeled congeners **1**. Similar to the parent ligands **1**, the labeled derivatives **5** and **10** exhibited single sets of signals, confirming average C_3-symmetry on the NMR scale. Moreover, the diastereotopic protons C−C^{1}H$_2$−O and −C^{1}H$_2$CO− of the chiral derivatives **5A**, **5L**, and **10A** were magnetically nonequivalent in $CDCl_3$ but equivalent (or nearly equivalent) in CD_3OD, as in the parent ligands **1**. The magnetic nonequivalence of these protons was

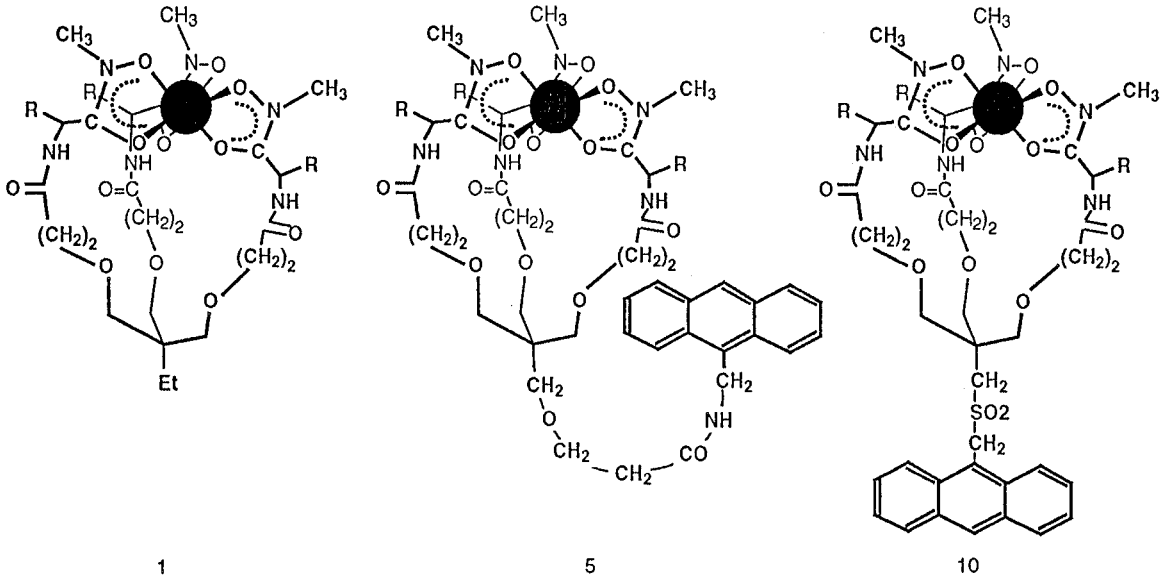

Figure 1. Schematic representation of ferrichrome analogs **1** and of fluorescent ferrichrome analogs **5** and **10**.

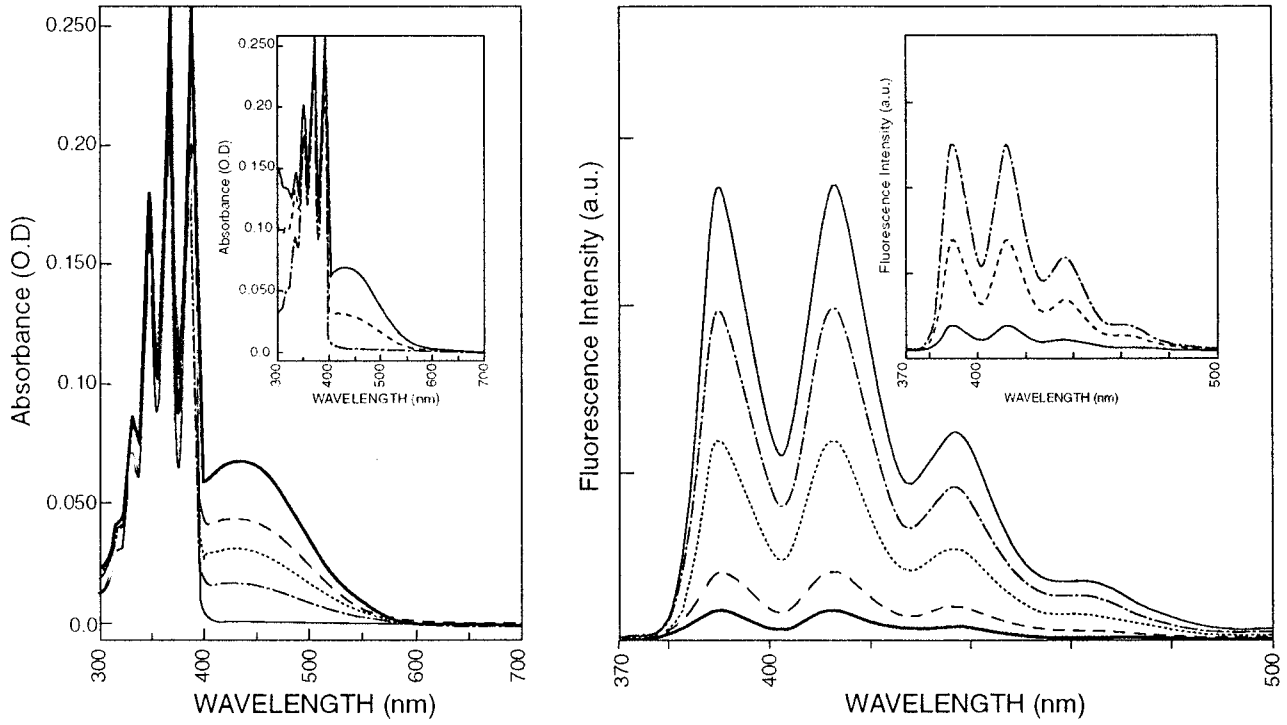

Figure 2. UV/vis (left) and fluorescence (right) iron(III)-titration experiments with labeled ferrichrome **5** analogs. Aliquots of stock solutions of ligand **5A** in methanol were treated with aliquots of methanolic solutions of $FeCl_3$ (0.0, —, 0.2 —•—, 0.6 ••, 0.8 — —, 1.0 equiv ▬) and diluted with methanol (80%)−0.1 N aqueous NaOAc (20%) to a final ligand concentration of 0.3 mM for UV/vis measurements and 6 μM for fluorescence measurements (final pH 7.4); UV/vis (left insert) and fluorescence (right insert) titration experiments of ligand **5A**−Fe(III) complex with EDTA. Solutions of ligand−**5A**−Fe(III), 1:1 complex (0.3 mM for UV/vis and 6 μM for fluorescence measurements) in methanol (80%)−0.1 N aqueous NaOAc (20%), were treated with aliquots of aqueous EDTA (0.0, —, 1.0, - -, 3.0 eq. —•—). All samples were equilibrated overnight before measurements were performed.

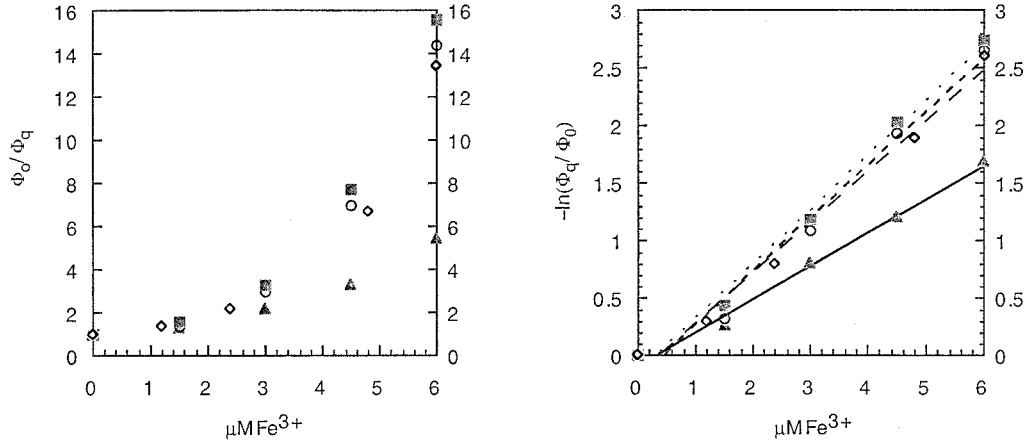

Figure 3. Plots for dynamic quenching (left) and static quenching (right) of the fluorescence of labeled ferrichrome analogs **5** (**5G**, ○; **5A**, ◇; **5L**, ■) and **10** (▲) by iron(III). The conditions were as described in legend to Figure 2.

attributed to the conformational constraints of the tripodal ion-binding cavity brought about by a network of intra- and interstrand H-bonds. The latter are only expressed in apolar solvents and are broken in polar solvents, as in the parent ligands **1**. Comparison between the chemical shifts of the backbone protons in the parent ligands **1** and their labeled derivatives **5** revealed pronounced up-field shifts (Table 1). These up-field shifts were particularly pronounced in the glycyl derivative **5G** and alanyl derivative **5A**, less so in the leucyl derivative **5L**. They were attributed to the proximity of the anthracenyl ring which bends toward the ligand backbone, as schematically depicted in Figure 1. The nonequivalence of the anthracenyl protons Ant-CH_2− in **5A** confirm this type of arrangement. In derivative **5L**, the isobutyl side chains screen the backbone, thereby diminishing the effect of the aromatic ring current. In the alanyl derivative **10A**, where the label is close to the anchor, such bending is prohibited, and the differences between the chemical shifts of **10A** and **1A** were negligible, except for the anchor's −C−C^1H_2−O protons which resonated at significantly lower field, probably because of the inductive effects exerted by the sulfone group.

UV/vis titration of the labeled derivatives **5** and **10** with $FeCl_3$ established the formation of Fe(III) complexes with a 1:1 stoichiometry, as reflected by their absorptions around 420 nm, which is characteristic for iron(III) trishydroxamates.[45] Moreover, the iron(III) complexes of the chiral derivatives **5A**, **5L**, and **10A** revealed two Cotton effects in the CD-spectra of opposite absolute sign in the visible region, with the positive Cotton effect appearing at a higher wavelength. These data demonstrate preferential Λ-cis configuration for the fluorescent derivatives, analogous to the chiral preference observed earlier for the parent compounds.[20]

These data confirm the close structural analogy between the iron-binding domain of the parent ligands **1** and their labeled derivatives **5** and **10**, both in the free state and complexed with iron. The structural analogy around the binding cavity is a prerequisite for recognition of the labeled derivatives by the microbial receptor sites. Subtle differences were, however, observed for the average location of the anthracenyl label in derivatives **5** and **10**. In the former, the label may bend toward the ion-binding domain, whereas in the latter the label may not reach the binding cavity. The latter structural differences were reflected in the compounds' photophysical properties.

All the labeled ligands, **5** and **10**, showed the characteristic absorption maxima of anthracene at 333, 348, 366, and 386 nm (ϵ = 2430, 4850, 7150, and 6610, respectively), and high fluorescence intensity with maxima at 395, 412, 435 and 464 nm when excited at 348 nm. Upon titration with iron(III), the molecules' fluorescence intensity decreased with increasing iron-hydroxamate absorption in the UV/vis spectrum (Figure 2). The observed fluorescence quenching, ϕ/ϕ_o, was not linear with quencher (iron(III)) concentration, and thus failed to obey the Stern-Volmer model of dynamic quenching. However, the $\ln\phi/\phi_o$ values were linear with quencher concentration, in agreement with the Perrin model of static quenching, where immobilized quenchers act over a significant distance (Figure 3).[44] The fitting of the quenching data to the Perrin model may be rationalized by assuming that (i) all added quencher is bound to the ligand, and (ii) the effect of the bound iron on the chromophore's fluorescence depends on the probability of the chromophore lying within the quencher's active sphere.

a. Dynamic quenching (Stern−Volmer Model)

$$^1M^* + {}^1Q \rightleftarrows {}^1(M.Q)^*$$

$$\frac{\phi^{FM}}{(\phi^{FM})^0} = \frac{1}{1 + k[Q]}$$

b. Static quenching (Perrin Model)

$$^1M + {}^1Q' \rightleftarrows {}^1(M.Q)' \rightarrow {}^1(M.Q)^*$$

$$\frac{\phi^{FM}}{(\phi^{FM})^0} = e^{-k'[Q]}$$

The addition of EDTA to solutions of the ligand−**5**−Fe(III) complex caused release of the hydroxamate-bound iron(III), as evidenced by the absorption decrease at 430 nm, and resultant gradual recovery of the fluorescence intensity (Figure 2, inserts).[46] These observations demonstrate that fluorescence quenching occurs predominantly, if not exclusively, intramolecularly.

Some differences in the fluorescence-quenching properties of the two types of derivatives, **5** and **10**, were observed. The fluorescence-quenching efficiencies k' in the Perrin equation for the leucyl-, alanyl-, and glycyl derivatives **5L**, **5A**, and **5G**, respectively, were almost identical (4.75×10^{-5}, 4.39×10^{-5}, and 4.63×10^{-5} M^{-1}, respectively). However, the quenching efficiency of the alanyl derivative **10A** was substantially lower, with a value of 2.84×10^{-5} M^{-1}. This illustrates the effect of the proximity (or accessibility) of the label to the iron(III) hydroxamate on the quenching process.

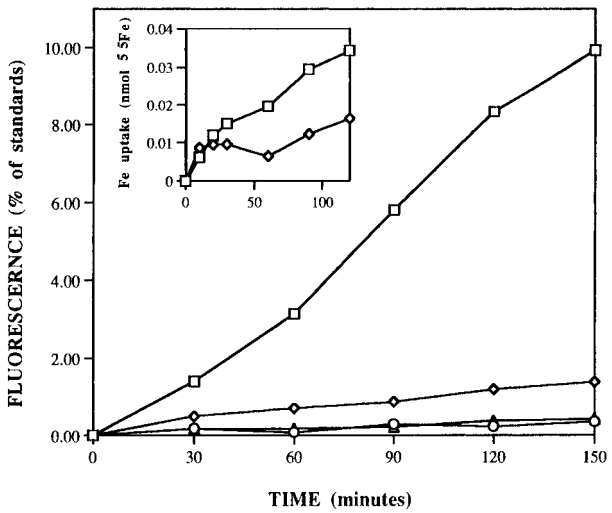

Figure 4. Appearance of anthracene fluorescence (λ_{exc} = 375 nm, λ_{em} = 415 nm) in the culture media of *Pseudomonas putida* JM218 upon treatment with labeled ferrichrome analogs **5G** and **5A** in the absence (**5G**, □; **5A**, ◇) and presence (**5G**, ○; **5A**, △) of NaN_3 as inhibitor. Insert: ^{55}Fe uptake with the ferrichrome analogs **5G** (□) and **5A** (◇).

A priori, fluorescence-quenching of anthracene by the iron(III)-hydroxamate chromophore could occur by heavy-atom-induced intersystem crossing, energy transfer, or electron transfer. Indirect evidence from our laboratory[43] as well as others[31,32,47] support the involvement of electron transfer in such processes. Earlier studies also seem to suggest that close contact between the components is advantageous for electron transfer.[48] The higher quenching efficiency in **5**, where the fluorophore can reach the iron(III) center, than in **10**, where the approach of the fluorophore to the iron(III) center is sterically prohibited, may reflect the contribution of electron transfer to the observed anthracenyl quenching processes.

Microbial Activity. Incubation of *P. putida* JM218 with the iron(III) complex of the labeled glycyl derivative **5G** resulted in the appearance of anthracene fluorescence in the cultures growth media. (As emphasized in the Experimental Section, the organisms were removed by centrifugation before measuring fluorescence.) This fluorescence was drastically reduced by the addition of NaN_3, an inhibitor of energy-dependent processes (Figure 4), or by the addition of natural ferrichrome as a competitor (data not shown). Incubation of *P. putida* JM218 with the alanyl derivative **5A** failed to induce any significant fluorescence (Figure 4). These experiments were complemented by ^{55}Fe-uptake experiments (Figure 4, inserts). Again, derivative **5G** proved superior to derivative **5A** in facilitating ^{55}Fe uptake. NaN_3 negated ^{55}Fe(III) uptake by both compounds. In contrast to the behavior of *P. putida*, incubation of *P. fluorescens S680*, or *P. fluorescens WCS3742* with **5G** or **5A** did not result in the generation of fluorescence in the culture media (Figure 5).

These results indicate that the labeled glycyl derivative **5G** acts as a specific agonist,[42] delivering iron(III) to the microorganism in an energy-driven process via a ferrichrome-specific iron(III) uptake system, then returning to the medium. The intactness of the released **5G** molecule is indicated by the quenching of its fluorescence upon addition of iron(III).

(46) Although the binding constants of hydroxamate siderophores to iron(III) are higher than those of EDTA (log K ~30 and 25, respectively), the apparent binding constant of the synthetic ferrichrome analogs **5** is comparable to that of EDTA under our experimental conditions, with pFe values of 15. EDTA may thus effectively compete with the ferrichrome analogs for iron(III).

(47) Nakamura, T.; Kira, A.; Imamura, M. *J. Phys. Chem.* **1983**, *87*, 3122−3125.

(48) Donckt, E. V.; vanVooren, C. *J. Chem. Soc. Faraday Trans. I* **1978**, *74*, 827−836.

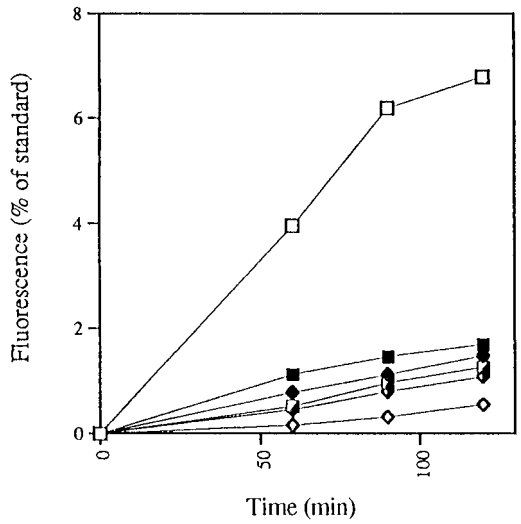

Figure 5. Appearance of anthracene fluorescence (λ_{exc} = 375 nm, λ_{em} = 415 nm) in the culture media of *Pseudomonas putida* JM218 upon treatment with labeled ferrichrome analogs **5G** (□) and **5A** (◇). Anthracene fluorescence (λ_{exc} = 375 nm, λ_{em} = 415 nm) in the culture media of *Pseudomonas fluorescens* S680 and *Pseudomonas fluorescens* WCS3742 upon treatment with labeled ferrichrome analogs **5G** (■ and ◪, respectively) and **5A** (◇ and diamond with right half shaded, respectively).

Derivative **5A** failed to deliver iron(III), acting as an antagonist[42] and remaining bound to the membrane as an intact complex. These results are in full agreement with our earlier findings that the glycyl-based ferrichrome analog **1G** functions as an iron-(III) carrier in *P. putida* JM218, whereas the corresponding alanyl derivative **1A** merely acts as an inhibitor of the natural ferrichrome by binding to the corresponding membrane receptor.[23] They further suggest that the synthetic ferrichrome analogs behave as shuttles and demonstrate that the presence of the rather bulky anthracene residue does not compromise the analogs' microbial activity.

Conclusions

Fluorescently labeled biomimetic analogs of the ferrichrome siderophore were prepared by applying a modular strategy of design and synthesis. These analogs possessed three crucial elements: hydrophilic cavities for iron binding, molecular envelopes for receptor recognition, and projecting fluorescent labels for signaling. In these assemblies, the labels did not interfere with either the ligands' iron-binding processes or with the complexes' microbial activity. Iron binding of these molecules caused quenching of their labels' fluorescence. Quenching was more efficient when the label could approach the iron-binding domain and is likely to involve electron transfer from the chromophore to the metal ion. The bioactive derivatives of these fluorescent compounds can therefore serve as versatile biological probes. They enabled us to monitor optically microbial iron-uptake processes and to trace the fate of the iron carriers after iron delivery. Concentrating on *P. putida* as an indicator organism, we demonstrated that the behavior of the labeled derivatives parallel that of the nonlabeled analogs, with the added benefit of signaling iron delivery via the appearance of fluorescence in the culture media. Moreover, these compounds were found to exhibit high specificity by distinguishing between different *Pseudomonas* species. This high specificity, and the possibility of incubating cultures with a series of differently labeled siderophore analogs that fit a given species' characteristic range of receptors and thereby provide a uniquely defined microbial "fingerprint", encourage the consideration of fluorescent analogs as diagnostic tools for the detection and identification of microorganisms. The energy dependence of such siderophore-based, diagnostic methods guarantees their uniqueness to live organisms, in contrast to DNA probes, which fail to distinguish between live and dead cells. Current investigations are aimed at preparing differently labeled siderophore analogs and applying them to the study of iron metabolism by fluorescence-imaging methods.[49,50] In addition, replacement of the fluorescent labels with toxic residues is envisioned to provide antimicrobial agents.

Acknowledgment. The authors thank Mrs. Rahel Lazar for her skillful technical assistance and the Israel Science Foundation and Edith Reich Foundation for financial support. A.S. is the holder of the Siegfried and Irma Ullman Professorial Chair.

JA9610646

(49) Because of the small size of bacteria, fluorescence microscopy of bacterial cultures (even at 1000× magnifications) does not enable distinguishing between fluorescence inside and outside the organisms and is thus of little diagnostic value with regards to the fluorescent siderophore analogs described here. In contrast to bacteria, fungi lend themselves to fluorescence microscopy studies. The latter possibilities are under current investigation.

(50) Ardon, O.; Nudelman, R.; Weizman, H.; Hadar, Y.; Libman, J.; Shanzer, A. *Preliminary results*, **1996**.